Study of the Hydroxyl Ion in Water. A Combined Quantum Chemical and Statistical Mechanical Treatment

Jose Manuel Hermida-Ramón* and Gunnar Karlström

Department of Theoretical Chemistry, Chemical Center, University of Lund, P.O. Box 124, S-221 00 Lund, Sweden

Received: December 19, 2002; In Final Form: April 23, 2003

A combined quantum mechanical−statistical mechanical method has been used to study the behavior of the hydroxyl ion in water. The system is divided into three parts, a quantum core (the ion), 89 classical water molecules, and a dielectric continuum. The water molecules are represented using a polarizable potential. The first solvation shell consists of four water molecules, two linked by hydrogen bonds to the oxygen of the ion and the other two linked to the hydrogen of the ion. The intermolecular distances obtained are in the same range as those in previous calculations. The intramolecular bond length in the ion decreases by 0.09 au upon solvation relative to the gas-phase value.

1. Introduction

In the last years, the use of a combination of statistical mechanical and quantum chemical ab initio methods to describe the interactions in solution has become more frequent.[1−7] Although the basis of this method is well established[8−10] (the system is divided in two subsystems, one containing the chemically interesting atoms and the other the bulk system), there is no accepted strategy to employ in these studies. The complexity of the interactions and the dependence on the inclusion of many molecules in the treatment have led to many ways of balancing between high-level theoretical treatment of a few molecules with a computationally less-demanding treatment of many molecules. This kind of method is important for systems in which the solvation is of relevance for the geometric and electronic structure. The development of a combined quantum mechanical−statistical mechanic method is important by itself because it constitutes a suitable theoretical tool that allows us to study large systems with a high degree of accuracy.

The hydroxyl ion is one of the most common ions in water, and it participates in many important reactions of chemical and biochemical interest. The presence of this ion leads to a number of interesting and rather unique properties of water[11] by forming hydroxyl ion−water clusters of different sizes. To study the hydration of a hydroxyl ion by a combined quantum chemical−statistical mechanical approach is a difficult task due to the very strong coupling between the classical and quantum systems. Special techniques are necessary to avoid the strong coupling leading to computational divergences. Recently, several theoretical studies have been made with the purpose of illuminating the cluster structure[12−17] and properties[3,18,19] of the hydroxyl ion in water. Some of these studies[12,14,17] suggest a first coordination shell of the OH^- ion of three water molecules. Others, however, predict a first coordination shell of two,[16] four,[18,19] or five[20] water molecules. It has been pointed out by Turki et al.[14] that the coordination number obtained will depend on whether the nonadditive contributions are considered. Most of the mentioned studies are performed for small clusters of water, and only a few[3,16,18,19] have been made using a statistical method. Among those, only Tuñon et al.[3] have employed a combined quantum mechanical−statistical mechanical method. That study was focused on the proton transfer between OH^- and water, and a nonpolarizable potential was used to represent the solvent water molecules. As far as we know, there is not any study in which the geometry of the hydroxyl ion has been optimized using a combined quantum mechanical−statistical mechanical method.

In the present work, we have applied a combined quantum mechanical−statistical mechanical method (QMSTAT) on a system composed of a quantum chemically described hydroxyl ion surrounded by 89 classically described water molecules. In the next section, we briefly describe the method, and in the following sections, the results and conclusions are presented.

2. Method and Computational Details

In the applied approach, the kernel system (the hydroxyl ion) is embedded in a spherical cavity in a dielectric containing a number (89 in this work) of classically described water molecules. Each of the classical water molecules is described by four point charges and three polarizabilities calculated using a multicenter multipole expansion.[5] The local charges and polarizabilities used to describe the electrostatic, induction, and dispersion interactions between the water molecules are a simplification of the more complex NEMO approach.[21] The energy calculation needs to be solved self-consistently also for the classical system because of the polarizabilities associated with the classical atoms. The expressions for the repulsion and dispersion contributions are the same as those for the NEMO model.[22,23] The same charges and polarizabilities are also used to model the interaction between the water molecules and the quantum mechanically described OH^-. For a detailed explanation of the QMSTAT model and the coupling between the different parts of the system, the reader is directed to refs 5−7. In this section, we will only describe the general ideas of the calculations and the changes introduced in this approach as a consequence of the study of a new system.

The quantum chemical calculations are performed on the Hartree−Fock level of approximation, and the effect of the classical molecules on the quantum system is introduced in the one-particle Hamiltonian matrix describing the quantum system.

10.1021/jp027770c CCC: $25.00
Published on Web 06/06/2003

In practice, this means that these matrix elements are modified because of the presence of the potential and generalized field from the charges and dipoles in the classical system. The dispersive coupling is added as a damped $1/r^6$ term acting between the atoms. To parametrize the model, the optimized ab initio self-consistent field (SCF) geometry of the water−hydroxyl ion complex was calculated. A line joining the oxygen of the ion and the hydrogen of water was used as one of the coordinate axes, and the SCF energy for the geometries obtained by small displacements along that line were calculated. All calculations were performed with an atomic natural orbitals (ANO) basis set[24] constructed from 10s, 6p, and 3d functions, which are contracted to 4s, 3p, and 1d on oxygen and a 6s4p basis set contracted to 3s and 2p on hydrogen. The intramolecular geometry of both molecules was fixed for all calculations. Thus, the bond distance of the hydroxyl ion was 1.783 au (the optimized value at SCF level), and the geometry of the NEMO approach[5] was used for water. The ab initio energies were calculated with the MOLCAS package.[25] Using the parameters of the above-mentioned QMSTAT model for water[5] as a starting point together with the dimer ab initio energies, we obtained the undetermined parameters in the intermolecular potential used in the QMSTAT model for the new system.

In the QMSTAT model, the charge density of the kernel is expanded into a multicenter multipole expansion.[26,27] The interaction between these multipoles and the classical molecules is used to describe the electrostatic and inductive coupling between the classical and the quantum systems.

Induced dipoles will be produced by the mutual polarization between the classical and quantum molecules. These dipoles will be obtained in a self-consistent way, together with the self-consistent field of the density in the quantum molecule.

To calculate the repulsion between the classical and quantum systems, each classical molecule is imbued with a wave function represented by a set of orbitals. When the distance between a classical molecule and the quantum molecule is smaller than a cutoff (7.7 au), a correction describing the exchange repulsion between the classical and the quantum molecule is included in the one-particle Hamiltonian describing the kernel. Thus, for two unperturbed orbitals, i,j, of the quantum system, the one-particle Hamiltonian will be corrected by

$$h_{ij}^{\text{correct}} = h_{ij}^{\text{unpert}}(1 + r_{ij}) \tag{1}$$

where h_{ij}^{correct} and h_{ij}^{unpert} are the corrected and unperturbed Hamiltonians, respectively. The parameter r_{ij} depends on the overlap between the wave functions of the quantum system and the wave function corresponding to the classical molecules. Thus, the contribution to r_{ij} from an occupied orbital k on the classical molecule is defined by

$$\Delta r_{ij} = \varphi(k)\sum_{m,n}[S_{ik}s_{jk(m,n)} + S_{jk}s_{ik(m,n)}]d_{(m,n)} \tag{2}$$

where $\varphi(k)$ is the orbital energy for an orbital k in the classical molecule and $d_{(m,n)}$ are exchange repulsion parameters that multiply the overlap between the orbitals. A value of −0.012 01 for all $d_{(m,n)}$ parameters gives a good agreement between the fitted and the quantum chemically calculated potential energy surfaces. S_{ik} is the overlap between orbital i in the quantum system and occupied orbital k in the classical system. $s_{jk(m,n)}$ is the contribution to this overlap from basis functions centered on atom of type m in the quantum system and atom of type n in the classical system.

TABLE 1: Parameters (hartree^{-30} Bhor) for the Non-Lennard-Jones Repulsive Term (eq 3)[a]

species	parameters
O−H	2.474 87
O−O	3.779 45
H−H	2.435 00
H−O	2.834 59

[a] The first label atom is the quantum atom, and the second is the classical atom.

TABLE 2: Effective Charges (au) and Diagonal Elements (au) of the Quadrupole Moment Tensor of the Hydroxyl Ion

	q_e	Q_{xx}	Q_{yy}	Q_{zz}
H	−0.7100	−0.3269	−0.4111	−0.4415
O	−7.2891	−5.9702	−6.4464	−6.6174

A short-range repulsive term of the form

$$\left(\frac{c_{ij}}{R_{ij}}\right)^{30} \tag{3}$$

has also been included in the potential to avoid too close encounters. The values of the c_{ij} parameters are given in Table 1. This extra repulsion is necessary to prevent the calculations on the composite system from diverging. To improve the description of the hydrogen bond between the quantum oxygen and the classical hydrogen, an extra term was introduced. This expression has the following form:

$$\left(\frac{1.7832}{R_{\text{OH}}}\right)^{5.5} \tag{4}$$

Such a term may, for example, include the contribution due to the interaction between the charge of the ion and the hyperpolarizability or octopole moment of the water molecules. These interactions are not described by any other term in the model. A Tang and Toennies[28] damping function was introduced in the dispersion term between the quantum and the classical molecules. The damping parameters for each atom are obtained from the expectation value of r^2 for the electrons assigned to the atom in the NEMO procedure. The expressions used to calculate these parameters, as well as the corresponding water parameters, are given elsewhere.[29] The parameters for the hydroxyl ion are given in Table 2. A damping function was applied to the field from the classical molecules on the quantum molecule. This function was

$$(1 - \mathrm{e}^{-(0.51R_{\text{Q-Cl}})})^4 \tag{5}$$

$R_{\text{Q-Cl}}$ is the distance between the quantum site and the classical atom.

A Monte Carlo simulation of 100 000 steps, after equilibration, was performed. In each a step, a small rotation and translation of each molecule is made, and every 80th step, a configuration is saved. A total of 1250 configurations have been stored. These are obtained using the SCF gas-phase geometry of the hydroxyl ion. A geometry optimization of the hydroxyl ion was performed. The effect of a geometry change, λ, in the hydroxyl ion can be determined by calculation of the energy of the system using the deformed geometry for the ion

$$\Delta G^{\lambda} = -RT\ln\left[\sum_{i}^{N}\frac{\mathrm{e}^{-\beta\Delta U_i^{\lambda}}}{N}\right] \tag{6}$$

where N is the number of configurations, 1250; ΔU_i^{λ} is the

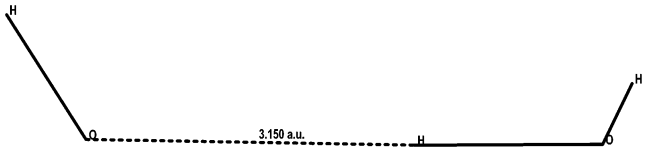

Figure 1. SCF-optimized geometry of the water−ion dimer.

difference in energy between the system with the gas-phase geometry in the *i*th configuration and the system with the λth deformed geometry in the same configuration. The ΔG^{λ} for a set of deformed geometries lead to a energy curve for the ion, and the optimized geometry can be obtained. Once a minimum is obtained with this procedure, a new QMSTAT simulation is performed using the new geometry as the geometry of the kernel system. This simulation gives a new set of conformations for a new optimization step. This procedure will be repeated until convergence is achieved. A more detailed explanation of this optimization procedure is given in ref 6.

3. Results and Discussion

3.1. Dimer Structure. The ab initio optimized geometry of the water−hydroxyl ion complex is shown in Figure 1. There is one significant difference between the geometry showed in this figure and the geometries calculated with ab initio methods in other studies,[13−15,17,30] and that is the value of the intermolecular distance between the oxygen atom of the ion and the hydrogen atom of water. This distance is around 0.45 au longer than the distance obtained with correlated calculations.[30] However, those calculations were performed with flexible molecules. We have done a MP2 optimization with nonflexible molecules (same intramolecular structure as QMSTAT values), and the intermolecular distance at MP2 level is 0.2 au shorter than the SCF value. These results point out that a substantial part of the difference with the results in other studies is because in our study we have been working with nonflexible water molecules. Especially, the relaxation of the structure of the water molecule is of importance for the intermolecular H−O distance. At least 50% of the observed difference is due to the structure of the water molecule. In the combined quantum mechanical−statistical mechanical model used here, it is not possible to use flexible solvent molecules. Thus, the parametrization will be performed using the properties of the minimum obtained for nonflexible molecules. The correlation in our model will be introduced in a phenomenological way. In this way, the largest and most important part of the intermolecular correlation will be handled. Taking all of this into account, the SCF energy can be considered as an acceptable reference for the QMSTAT parametrization. In Figure 2, the ab initio and QMSTAT energies for the optimized dimer and some geometries obtained by small changes of the intermolecular O−H distance are presented. It can be seen that the ab initio curve is flatter than the QMSTAT curve. Close to the minimum, the agreement is very good. The parametrized curve has a much larger slope for the geometries with a short intermolecular O−H distance than the ab initio curve. This was needed to avoid the possibility of the induction catastrophe that appears at short distances.

3.2. Structure of the OH Ion Solvation Sphere. The Monte Carlo simulation was performed at a temperature of 300 K. The cavity radius specifying the start of the continuum was calculated to around 19.3 au in the equilibrium process. The pair correlation functions, $g(r)$, obtained from the QMSTAT simulation are displayed in Figure 3, and they show the most probable values for the distances between quantum and classical atoms. In the labels in this figure, as well as in the rest of the manuscript, the

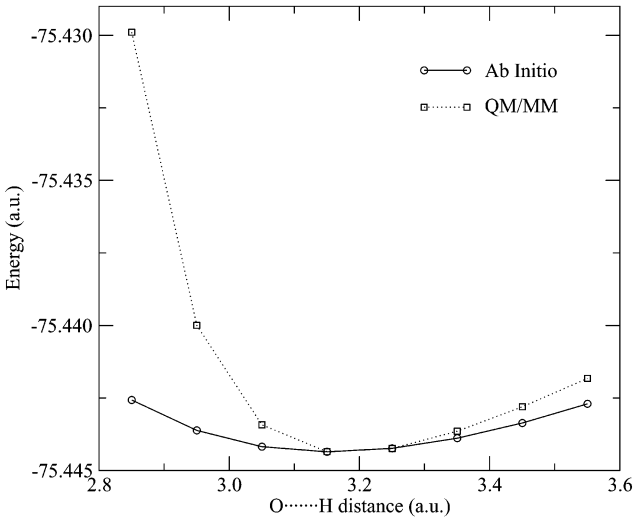

Figure 2. Energy of the water−ion dimer in the optimized geometry as a function of the OH distance.

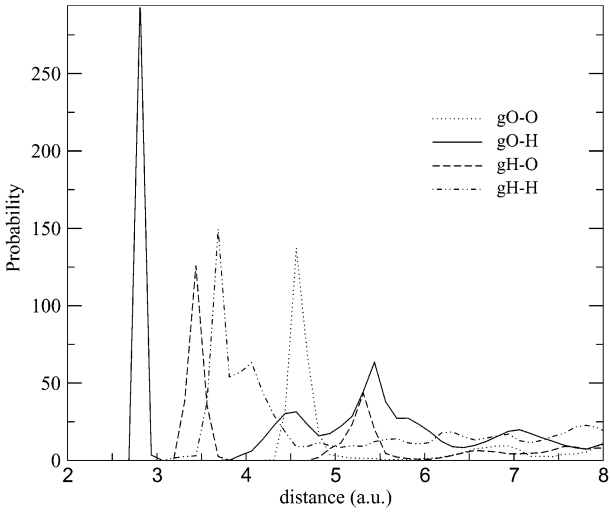

Figure 3. Pair correlation functions in arbitrary units as a function of interatomic distance for the different ion−water pairs. Labels are denoted quantum atom−classical atom.

first character labels the quantum atom and next the classical one. To facilitate the assignment of the different peaks in the correlation functions and to obtain a better understanding of the internal structure of the ion solvation, we have chosen to present four different snapshots from the simulation in Figures 4−7. These figures show the hydroxyl ion and the closest water molecules (water molecules with an oxygen atom within a radius of 8 au from the oxygen of the hydroxyl ion). The conformations represented in Figures 4, 5, 6, and 7 appear after 16 000, 32 000, 48 000, and 96 000 steps, respectively.

The highest peak in the correlation functions corresponds to the distance between the quantum oxygen and one of classical hydrogen atoms on the two closest water molecules. There are two other peaks in the correlation function of the O−H pair. One is quite broad and is positioned at a distance around 4.6 au. This distance is consistent with the O−H distance to molecule III (see Figures 4−7), and it matches also with the distances to both of the hydrogen atoms in molecules IV and V. In some of the conformations, it matches only with one of these molecules (see Figure 4) and in others with both of them (see Figure 5). This peak arises from the combination of all these distances, and because they have large fluctuations, it appears as a rather broad peak. Partly overlapping with the

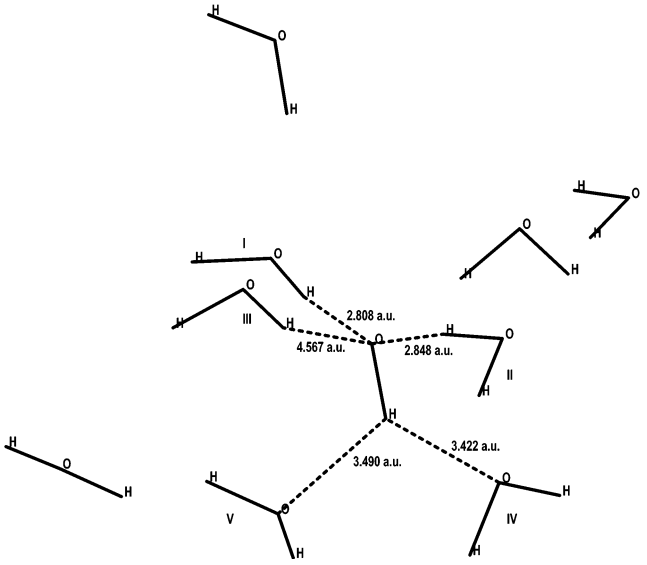

Figure 4. Configuration of the ion and its closest water molecules after 16 000 steps of the simulation (see text).

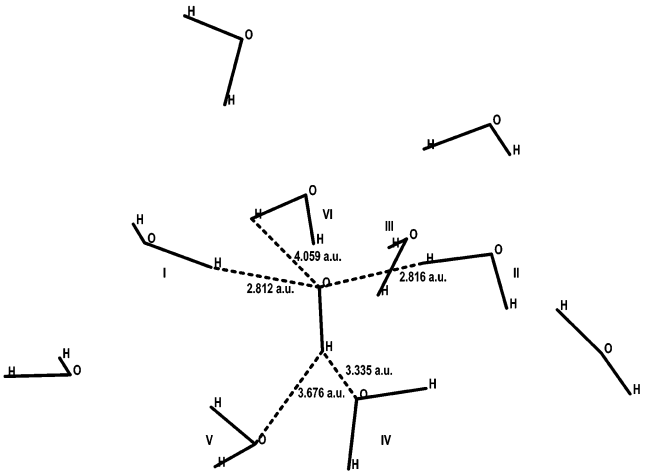

Figure 5. Configuration of the ion and its closest water molecules after 32 000 steps of the simulation (see text).

previous one but at larger distances, 5.4 au, there is another peak. It corresponds to the distances between quantum oxygen and the hydrogen atoms of molecules I and II that do not participate in the hydrogen bonds.

The correlation function for the H−O pair has two pronounced peaks. One is at a short distance, 3.4 au, consistent with the distance between the quantum hydrogen and the classical oxygens of molecules IV and V. It is interesting to note that the nearest neighbor of the quantum hydrogen is an oxygen, despite the fact that the OH ion is negatively charged. The peak at a larger distance (5.3 au) is in good agreement with the distances to the oxygens of molecules I and II.

There is only one peak (at 4.6 au) in the O−O pair correlation function. This value agrees with the value of the distance between the quantum oxygen and the classical oxygen of molecules I, II, IV, and V. The lack of other peaks shows that the distance to the oxygen in molecule III (Figures 4 and 5) is not well defined and may change within a large range of values.

The H−H correlation function has two close peaks. The first and highest peak occurs at 3.7 au, and the other one is found at 4.1 au. The distances between the quantum hydrogen and the nearest classical hydrogen in molecules I and II are in very good agreement with the first value. The distances between the

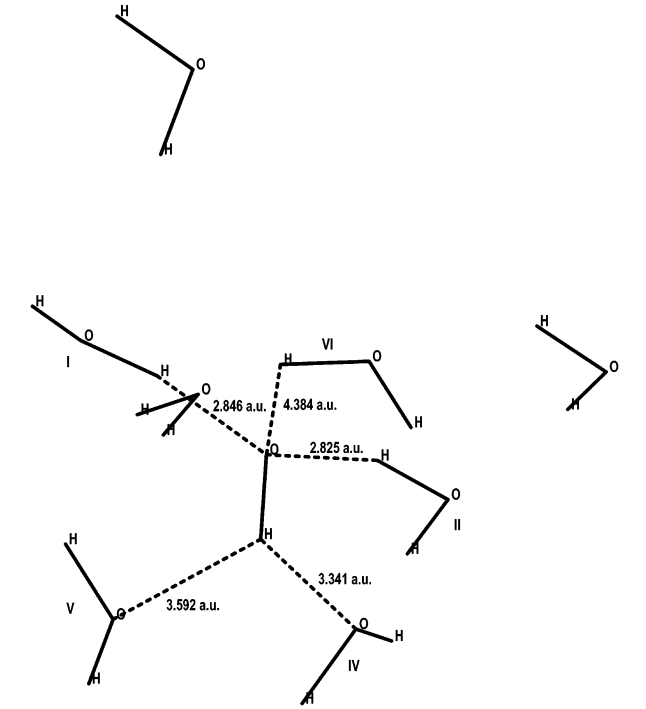

Figure 6. Configuration of the ion and its closest water molecules after 48 000 steps of the simulation (see text).

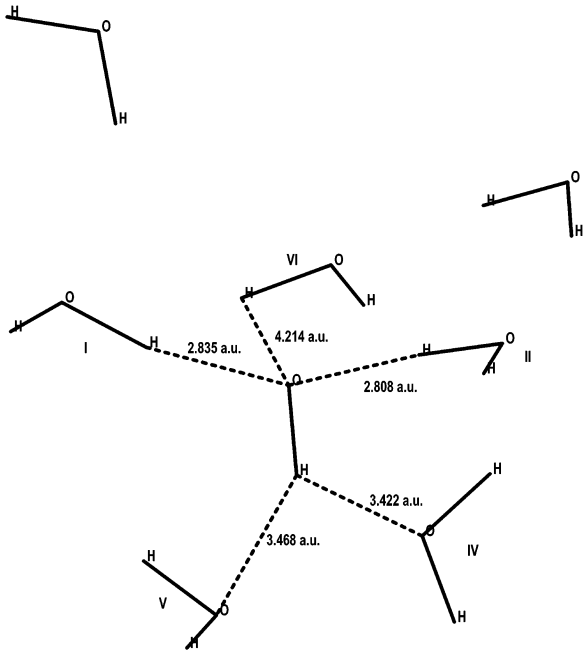

Figure 7. Configuration of the ion and its closest water molecules after 96 000 steps of the simulation (see text).

quantum hydrogen and the hydrogens of molecules IV and V vary between 3.7 and 4.4 au. These values will contribute to the peak at 3.7 au, but they also explain the existence of the broad peak at 4.1 au. The hydrogens in molecules I and II that are most distant from the quantum hydrogen have no defined positions.

The structures shown in Figures 4−7 give an idea of the position of the closest OH^- neighbors along the simulation. There are four water molecules (molecules I, II, IV, and V) in a rather fixed position during the complete simulation. These molecules have a hydrogen bond with the ion. There is, however, one molecule (molecule III) that also has a hydrogen bond with the ion, but it does not have a fix position during the simulation.

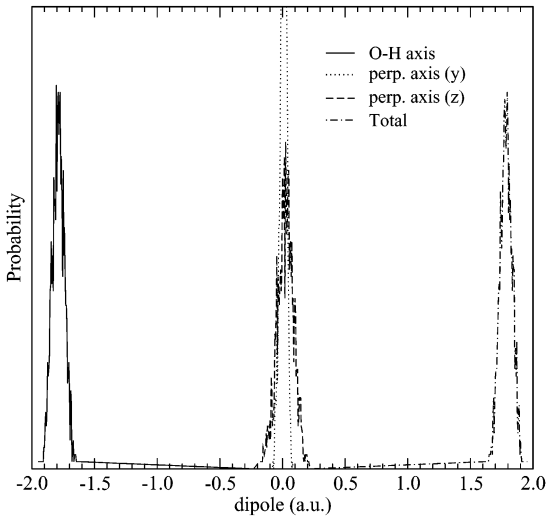

Figure 8. Unnormalized probability distribution of the total dipole moments and the different components of the induced dipole moment of the ion in au.

In Figure 4, molecule III is in the front and at a distance of 4.6 au, while in Figure 5, it has moved to larger distances, and another molecule (molecule VI, in the back) has formed a hydrogen bond with the ion. In the rest of the simulation, this molecule (molecule VI in Figures 6 and 7) maintains the hydrogen bond, but its position is rather flexible, and the molecule can be found at a wide range of distances. The freedom in the position of this molecule is also indicated by the correlation functions. Thus, there is not any peak in the O−O correlation function that suggests a fixed position for this molecule.

There exist several studies in which the number of water molecules that form a hydrogen bond with the oxygen atom of the ion have been calculated. One of these studies[20] proposes five water molecules; other studies predict four,[18,19] three,[12,14,17] and two[16] molecules of this type. Turki et al. pointed out that the nonadditive induction in the intermolecular interaction decreases the coordination number from four to three. Their calculations, as most of the others, were done for small clusters. A study[16] was performed for a solvent taking into account the nonadditive induction contribution using a many-body potential. This calculation is in agreement with our result and gives a coordination number of two. This indicates that it is necessary to introduce the nonadditive effects not only in the quantum system but also in the classical solvent to obtain reliable results for the solvation of the hydroxyl ion. One should also keep in mind that the strength of the different hydrogen bonds is different (the two short ones between the quantum oxygen and the classical hydrogens are very strong, whereas the others are much weaker) and that the number of hydrogen bonds depends on the definition used.

In Figure 8, an unnormalized probability distribution of the total dipole moment, as well as the different components of the induced dipole moment, in the hydroxyl ion is shown. The induced dipoles are almost parallel with the O−H bond, and the values for the perpendicular components are almost zero. We also note that the sign of the induced dipole is such that electrons flow from the hydrogen to the oxygen in the hydroxyl ion. This will increase the ionic character of the O−H bond and shorten the bond.

3.3. Structure of the Solvated OH Ion. To determine the geometry of the solvated ion, an optimization was performed using the method outlined above. The calculations predict a minimum for the hydroxyl ion in which the O−H bond is shortened by 0.089 au compared to the gas-phase distance (1.783 au). This new geometry was used as a new reference point to perform a QMSTAT simulation and a new optimization using the perturbation method. The geometry obtained in this second iteration changes by 0.0007 au relative to the geometry obtained in the first iteration, indicating that the result is converged. The calculated value shows the same trend that has been seen in previous studies,[13−15,17] but the magnitude of the shortening is 4 times bigger. Part of the difference can be because we are studying an ion in bulk water and the previous studies refer to small clusters. In these clusters,[13−15,17] the hydrogen of the ion has hydrogen atoms as closest neighbors; however, it can be seen in Figures 4−7 that the hydrogen in the ion has oxygen atoms as its nearest neighbors in our study; this circumstance will produce a larger electric field on the ion and thus bigger geometry changes. The influence of the solvent is likely to enhance the shortening of the distance seen in calculations on small clusters. Nevertheless, it is possible that our model predicts a too big change in the bond distance. We have performed calculations to obtain the optimized bond distance using two other models for the solvent. One of these was to employ a Langevin dipoles model;[10,31−33] the other was to utilize a polarizable continuum model (PCM).[34,35] The first method predicts a bond distance that is 0.005 au shorter than the gas-phase distance. A detailed explanation of the Langevin dipoles used model is given in a previous work.[33] Two optimizations were performed with the PCM model using the MOLCAS package.[25] In one of the optimizations, the standard Pauli radii were used for the atoms, and in the other, the standard Pauli radii were multiplied by 1.5. These optimizations give bond distances that are 0.0033 and 0.0027 au shorter than the gas-phase value. The results given by the Langevin dipole model and by the PCM model predict most likely a too small change for the interatomic distance.

4. Conclusions

A combined QM/MM method has been used to study the behavior of a hydroxyl ion in water. The model includes the nonadditive interactions not only in the quantum system but also between the classical water molecules and between the water molecules and the quantum system. A damping function has been used for the electric fields to prevent a polarization catastrophe.

The obtained results show a highly ordered first solvation shell composed of two water molecules bonded, by a hydrogen bond, to the oxygen atom and two water molecules linked to the hydrogen atom. The simulations show that another water molecule forms a "weak" hydrogen bond with the oxygen of the ion. This hydrogen bond is very long and flexible.

Previous studies predict a number of water molecules solvating the oxygen of the hydroxyl ion varying from two to five. Some of these studies are made on water clusters, and others do not take into account the nonadditive interactions in the system. These two factors seems to be important to obtain a good description of the solvation of the ion. The obtained intermolecular distances for the different pairs of atoms are in agreement with the results of previous calculations.

The QMSTAT model predicts that the ion intramolecular bond is 0.089 au shorter than the gas-phase value. This is between 4 and 5 times bigger than the ab initio results. However, it must be considered that the previous values are calculated for small clusters of water and that the predicted value is likely to be shorter in the bulk water. Even so, it is possible that the QMSTAT result corresponds to a too large change.

Acknowledgment. J.M.H.-R. thanks the "Ministerio de Educación, Cultura y Deporte" for award of research grant.

References and Notes

(1) Tongraar, A.; Rode, B. M. *J. Phys. Chem. A* **1999**, *103*, 8524.
(2) Elola, M. D.; Estrin, D. A.; Laria, D. *J. Phys. Chem. A* **1999**, *103*, 5105.
(3) Tuñón, I.; Martins-Costa, M. T. C.; Millot, C.; Ruiz-López, M. F. *J. Chem. Phys.* **1997**, *106*, 3633.
(4) Tuñón, I.; Silla, E.; Millot, C.; Martins-Costa, M. T. C.; Ruiz-López, M. F. *J. Phys. Chem. A* **1998**, *102*, 8673.
(5) Moriarty, N. W.; Karlström, G. *J. Phys. Chem.* **1996**, *100*, 17791.
(6) Moriarty, N. W.; Karlström, G. *J. Chem. Phys.* **1997**, *106*, 6470.
(7) Moriarty, N. W.; Karlström, G. *Chem. Phys. Lett.* **1997**, *279*, 372.
(8) Gao, J. In *Reviews in Computational Chemistry*; Lipkowitz, K. B., Boyd, D. B., Eds.; Plenum Press: New York, 1996; Vol. 7, p 119.
(9) Sherwood, P. In *Modern Methods and Algoriths of Quantum Chemistry*, Grotendorst, J., Ed.; NIC series, Vol. 1; John von Neumann Institute for Computing: Jülich, Germany, 2000; p 1.
(10) Orozco, M.; Luque, F. J. *Chem. Rev.* **2000**, *100*, 4187.
(11) Fehsenfeld, F. C. *Water, A Comprehensive Treatise*; Plenum Press: New York, 1972; Vol. 3.
(12) Tuñón, I.; Rinaldi, D.; Ruiz-López, M. F.; Rinaldi, J. L. *J. Phys. Chem.* **1995**, *99*, 3798.
(13) Xantheas, S. S. *J. Am. Chem. Soc.* **1995**, *117*, 10373.
(14) Turki, N.; Milet, A.; Rahmouni, A.; Ouamerali, R. O.; Moszynski, R.; Kochanski, E.; Wormer, P. E. S. *J. Chem. Phys.* **1998**, *109*, 7157.
(15) Pliego, J. R.; Riveros, J. M. *J. Chem. Phys.* **2000**, *112*, 4045.
(16) Vegiri, A.; Shevkunov, S. V. *J. Chem. Phys.* **2000**, *113*, 8521.
(17) Chaudhuri, C.; Wang, Y.-S.; Jiang, J. C.; Lee, Y. T.; Chang, H.-C.; Niedner-Schatteburg, G. *Mol. Phys.* **2001**, *99*, 1161.
(18) Tuckerman, M.; Laasonen, K.; Sprik, M.; Parrinello, M. *J. Phys. Chem.* **1995**, *99*, 5749.
(19) Tuckerman, M.; Laasonen, K.; Sprik, M.; Parrinello, M. *J. Chem. Phys.* **1995**, *103*, 150.
(20) Andaloro, G.; Palazzo, M. A.; Migliore, M. *Chem. Phys. Lett.* **1988**, *149*, 201.
(21) Wallqvist, A.; Karlström, G. *Chem. Scr.* **1989**, *29A*, 131.
(22) Wallqvist, A.; Ahlström, P.; Karlström, G. *J. Phys. Chem.* **1990**, *94*, 1649.
(23) Wallqvist, A.; Ahlström, P.; Karlström, G. *J. Phys. Chem.* **1991**, *95*, 4922.
(24) Pierloot, K.; Dumez, B.; Widmark, P. O.; Roos, B. O. *Theor. Chim. Acta* **1995**, *90*, 87.
(25) Andersson, K.; Baryz, M.; Bernhardsson, A.; Blomberg, M. R. A.; Boussard, P.; Cooper, D. L.; Fleig, T.; Fülscher, M. P.; Hess, B.; Karlström, G.; Lindh, R.; Malmqvist, P.; Neogrady, P.; Olsen, J.; Roos, B. O.; Sadlej, A. J.; Schimmelpfennig, B.; Schtz, M.; Seijo, L.; Serrano, L.; Siegbahn, P. E.; Stålring, J.; Thorsteinsson, T.; Veryazov, V.; Wahlgren, U.; Widmark, P. *MOLCAS*, version 5.0; Department of Theoretical Chemistry, Chemical Center, University of Lund: Lund, Sweden, 2000.
(26) Karlström, G. On the evaluation of intermolecular potentials. In *Proceedings of the 5th Seminar on Computational Methods in Quantum Chemistry*; van Duijnen, W. C., Nieuwpoort, P. T., Eds.; Laboratory of Chemical Physics, University of Gronningen: Gronningen, The Netherlands, and Max-Plank-Institut für Physik und Astrophysik; Institut für Astrophysik: Garching bei München, Deutschland, 1981; p 353.
(27) Karlström, G.; Linse, P.; Wallquist, A.; Jönsson, B. *J. Am. Chem. Soc.* **1983**, *105*, 3777.
(28) Tang, K. T.; Toennies, J. P. *J. Chem. Phys.* **1984**, *80*, 3726.
(29) Åstrand, P.-O.; Wallqvist, A.; Karlström, G. *J. Chem. Phys.* **1994**, *100*, 1262.
(30) Salvador, P.; Duran, M.; Dannenberg, J. J. *J. Phys. Chem. A* **2002**, *106*, 6883.
(31) Warshel, A.; Åqvist, J. *Annu. Rev. Biophys. Biophys. Chem.* **1991**, *20*, 267.
(32) Warshel, A. *Computer Modeling of Chemical Reactions in Enzymes and Solutions*; Wiley: New York, 1991.
(33) Hermida-Ramón, J. M.; Karlström, G.; Lindh, R. *J. Phys. Chem. B* **2002**, *106*, 7115.
(34) Miertus, S.; Scrocco, E.; Tomasi, J. *Chem. Phys.* **1981**, *55*, 117.
(35) Miertus, S.; Tomasi, J. *Chem. Phys.* **1982**, *65*, 239.